Materials Physics and Mechanics 42 (2019) 717-730 Received: January 24, 2019

THE IMPACT OF HIGH HEATING RATES ON THE AUSTENITIZATION PROCESS OF 18NiCrMo5 STEEL

A.G. Settimi[1*], D. Chukin[2], L. Pezzato[1], C. Gennari[1], K. Brunelli[1.3], M. Dabalà[1]

[1]Department of Industrial Engineering, University of Padova, Via Marzolo 9, 35131, Padova, Italy

[2]Nosov Magnitogorsk State Technical University, Avenue Lenin 38, 455000, Magnitogorsk, Russia

[3]Department of Civil, Constructional and Enviromental Engineering, University of Padova, Via Marzolo 9, 35131, Padova, Italy

*e-mail: alessio.settimi@gmail.com

Abstract. This paper is focused on the study of the effect of high heating rates on austenite formation of 18NiCrMo5 steel. The prior martensitic microstructure was characterized with scanning electron microscopy and Vicker micro-hardness. Then dilatometric tests were performed at 12 different heating rates (in the range of 100 - 3000°C/s), to evaluate the critical points and the key factor governing the austenite formation with high heating rates. After these tests, the microstructures obtained were analyzed by optical microscopy, scanning and transmission electron microscopy. The Ac_1 and Ac_3 temperatures initially increased with heating rate, reaching a maximum and then decrased. The formation of austenite from martensite, with low heating rates, was diffusive, whereas with high heating rates, it took place through a displacive mechanism. Moreover, a higher dislocation density characterized the austenite obtained with high heating rates.

Keywords: low alloyed steel, 18NiCrMo5, austenitization, heating rate, austenite, martensite

1. Introduction

Heat treatment of steels is a common procedure to obtain materials with the desired properties and structures. The first step for the vast majority of heat treatment, such as quenching, normalizing, annealing and surface hardening, is austenitization, which consists in the formation of austenite upon heating from a variety of prior microstructures [1]. For this reason, investigation on austenitization process is a very important topic from an industrial and scientific point of view. In fact, heating rate, homogeneity of austenite, and grain size of austenite influence the final microstructure and the mechanical properties of the materials [2]. However, only few works in literature are focused on the transformation of ferrite to austenite, whereas most of studies concern the austenite decomposition.

An important aspect to be considered for austenitization is the prior microstructure of the steel. Indeed, it was early realized that the formation of austenite is a structure-dependent process, and thus different initial microstructures play a key role on austenite formation process and the morphology of formed austenite as stated by Thibaux et al. [3]. Numerous studies were done on pure iron [4] and on steel with prior microstructure constituted by ferrite-lamellar pearlite [5] and by ferrite-spheroidized pearlite [6]. Other early studies included martensite [7] as starting microstructure for the formation of austenite. Austenite formation in low alloy steels with a ferrite-lamellar pearlite and ferrite-spheroidized pearlite prior microstructures, consists in a two stages process [8]. The first stage of the transformation is the pearlite dissolution, followed by the ferrite to austenite transformation.

http://dx.doi.org/10.18720/MPM.4262019_4
© 2019, Peter the Great St. Petersburg Polytechnic University
© 2019, Institute of Problems of Mechanical Engineering RAS

Each of these processes takes place by a nucleation and growth mechanism [9]. Regarding prior martensitic steel microstructure, Shinozaki et al. [10] found that acicular austenite arised from the elongated martensitic laths and/or packets. According to Kinoshita and Ueda [11], acicular austenite formation was enhanced by slow heating rate, low austenitizing temperature, and also by acicular prior microstructure [12].

An important aspect in the austenitization process concerns the study of the effect of high heating rates on austenitization mechanism and on the resulting microstructure. Indeed, in some industrial heat treatment application, *e.g.* induction hardening, the austenitazion occurs under rapid heating and very short time [13].

Castro Cerda *et al.* [14] showed that higher heating rates led to increase both the critical austenitization temperatures (in particular Ac_3) and the rate of austenite formation. However, if the prior microstructure is constituted by martensite, the mechanism is different. In fact, it was demonstrated that the critical points increase only for slow heating rates. At high heating rate it was found that critical points decreased and/or stabilized [15].

It is clear that austenitization process at high heating rates is an issue of great industrial interest. Indeed, at short heating times, incorrectly selection of the heating conditions can be the reason of significant errors during heat treatment [16]. For this reason, the development of proper prediction models is important in the design of induction heat treatment cycles, allowing better process control with the aim of producing customised-heat treated components. However, this phenomenon is more complex, depending both on thermal cycle parameters and on prior microstructures of the steel, and, therefore, requires a deeper knowledge in order to be industrially employed.

According to García de Andres *et al.* [17], dilatometry is a useful technique for the study of solid-state transformations, such as austenitization under continuous heating. Indeed, when a phase transformation occurs, the dilatometric curve provides information on change in atomic volume due to transformation as well as on thermal expansion characteristics. The data collected in most of the studies result from dilatometric experiment, where heating rates are limited to the range of 0.01 – 20 K/s. In some cases, the experiments considered heating rates up to 300 K/s as shown by Dykhuizen *et al.* [18]. The highest heating rate employed is 1000 K/s in the work developed by Katsamas [19].

The present paper is focused on the quantitative assessment of influence of the heating rate on the austenitization kinetics for a 18NiCrMo5 steel, which is widely used for components subjected to wear. This is an upgrade of a previous work carried out by Spezzapria *et al.* [20] on 39NiCrMo steel. In this work, 18NiCrMo5 steel was employed in order to reduce carbon diffusion during the various tests, exploiting the low carbon concentration of this steel. The as-received steel was heat-treated to develop a martensitic prior microstructure. Dilatometric tests were carried out using different heating rates in the 100-3000 K/s range. The microstructure characteristics were analyzed by means of optical, scanning and transmission electron microscopy. The experimental results were compared and evaluated to determine the key factors governing the austenite formation at high heating rates.

2. Experimental Procedure

The material used in this study was the steel 18NiCrMo5. Its chemical composition, measured by GDOES analysis, is given in Table 1 (in wt.%).

Table 1. Chemical composition of the 18NiCrMo5 investigated steel (mass.%)

C%	Si%	P%	Mn%	S%	Cr%	Mo%	Ni%	Al%	Cu%	Pb%
0.18	0.28	0.02	0.75	0.033	0.85	0.2	1.35	0.021	0.099	0.15

The tensile test specimens with a geometry of Fig. 1, were obtained by turning operations from a round bar with diameter 20 mm.

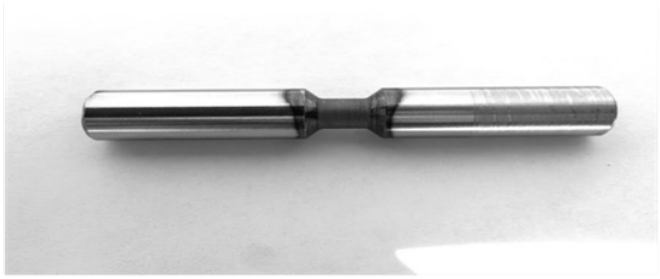

Fig. 1. Example of specimen employed in dilatometric tests

In order to remove the microstructure due to the previous heat treatments, all samples were normalized (heat treated at 1153 K for 1 hour and cooled in calm air). Then, the specimens were austenitized at 1123 K for 30 minutes and quenched in oil to obtain final microstructure of martensite. The microstructures of the samples were analyzed in a section coming from the edge of the specimens by scanning electron microscopy (SEM) with a JEOL JSM 6490LV and a LEICA™ Cambridge Stereoscan 440. Vicker micro-hardness (using Leitz ™ DURIMET hardness tester) measurements were performed using load of 200 g. Dilatometric tests were carried out by Gleeble 3500 thermo-mechanical simulation instrument. The Gleeble 3500 incorporates a closed-loop thermal system and a closed-loop hydraulic servo system under synchronous digital computer control, allowing an accurate temperature control as well as steep heating rates. Different heating rates were employed in this work (Table 2).

Table 2. Heating rates selected to perform dilatometric tests

Sample	1	2	3	4	5	6	7	8	9	10	11	12
Heating Rate [Ks^{-1}]	100	300	500	700	1000	1200	1500	1700	2000	2200	2600	3000

The test specimen was supported between two grips and heated by direct resistence heating. Cooling was accomplished in calm air with equal cooling rates for all samples. Dimensional change related to thermal expansion and phase transformation was measured along diameter at the center of the test specimen length with mechanical apparatus (LVDT extensometer), whereas temperature was measured by Type K thermocouple fixed to the surface of the specimen always at the center of the specimen length. The progress of austenite transformation during continuous heating was noted by means of the critical transformation points Ac_1 and Ac_3 determined from the resulting dilatometric curves [22]. Morover, the lever rule was applied to obtain the overall fraction of phase transformed as described by Kang *et al.* [23]. The microstructures after dilatometric tests at 100-300-1000-1700-2200-3000 K/s were analysed with OM (LEICA^{TM} DMRE), SEM and transmission electron microscope (TEM) (JEO 200CX operating at 160 kV). Thin foil specimens with 3 mm in diameter for TEM investigations were mechanically ground to 100 mm in thickness. Then, these specimens were electrochemically polished in solution of 90% acetic acid (CH_3COOH) and 10% perchloric acid ($HClO_4$) at ambient temperature using a twin-jet polisher (Struers Tenupol-5).

3. Results and Discussion

Prior Microstructures. Optical and SEM analysis were carried out in order to verifiy the real effectiveness of the heat treatment selected. Firstly, the microstructure of normalized samples was analyzed in order to verify the good quality of the normalizing treatment. The results are reported in Fig. 2.

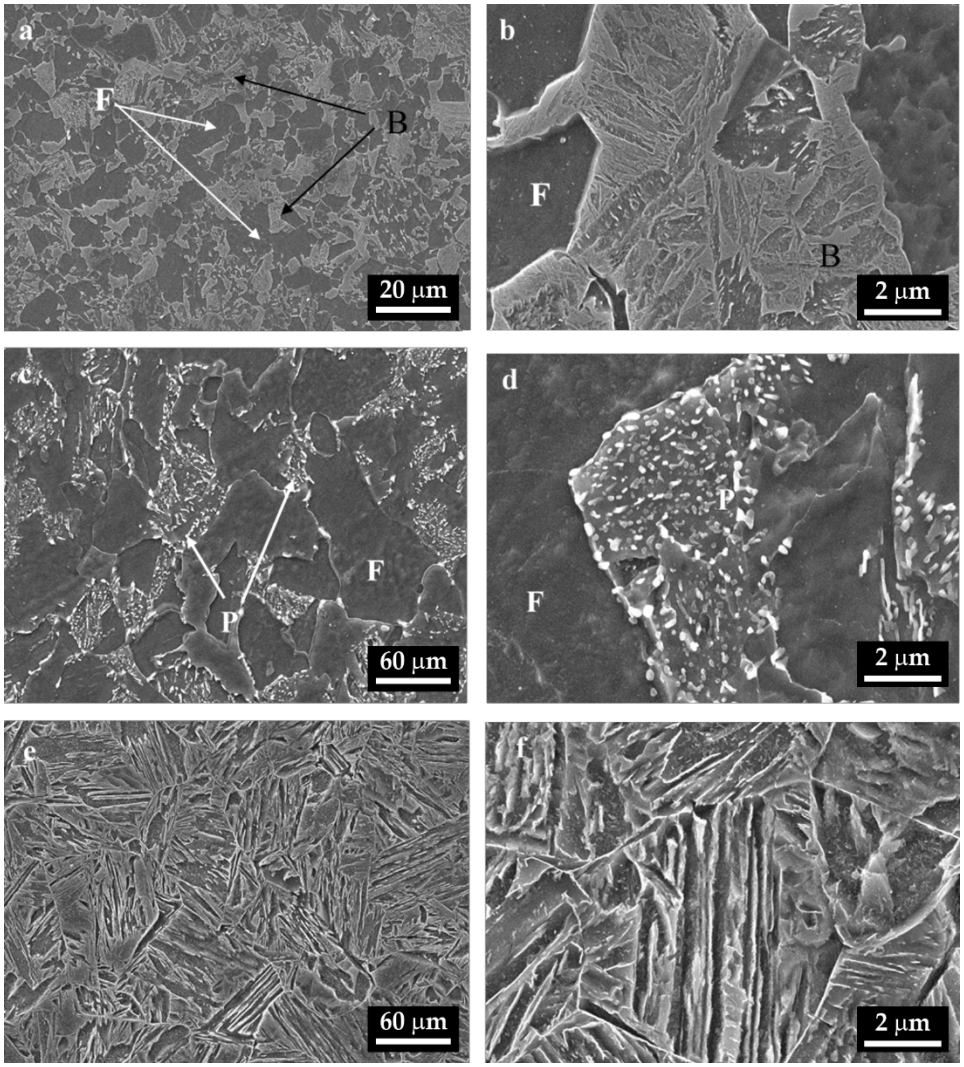

Fig. 2. Examples of SEM microstructures, before dilatometric tests, obtained with different heat treatments: (a-b) as-received sample, (c-d) normalized sample and (e-f) just-quenched sample. Etching with Nital 5%. F means ferrite, P means Pearlite and B means Bainite

The as-received samples were constituted by ferritic grains surrounded by bainitc areas (Fig. 2a and b). Compared to the normalized samples (Fig. 2c and d), which microstructure consisted of mixture of granular pearlite in matrix of ferrite, the as-received samples showed coarser and less uniform grain structure. After quenching treatment, the resulting microstructure consisted in "lath martensite" (Fig. 2e and f). This phase was composed by nearly parallel oriented plates which were separated by low angle boundaries. The transformation of prior austenite into lath martensite was characterized by grain subdivision on different lenght scale with three-level hierarchy in its morphology: lath, block and packet. In particular, the austenite grain broke down to several packets, each of them with internal extended parallel blocks. Each block was further subdivided by laths as stated by

Kitahara *et al.* [23]. However, some amount of retained austenite was present after quenching. This is visible as light-colored areas trapped between dark-colored martensite needles.

The high values of Vickers micro-hardness for quenched sample (Table 3) compared to that normalized, confirmed the effectiveness of the quenching conditions.

Table 3. Vickers micro-hardness of just-quenched and normalized sample before dilatometric tests. The coefficient of variation (CV) is defined as the ratio of standard deviation to mean value

Treatment	**Mean Vicker Hardness (HV)**	**Standard Deviation**	**CV (%)**
Normalizing	175	7	4 %
Quenching	512	23	4.5 %

Dilatometric tests. Dilatometric tests were conducted twice times for each heating rates. Figures 3(a), (b) and (c) show the radial displacement *vs.* temperature for all heating rates, where the linear regions represent the zones of thermal expansion without any phase transformations. The formation of austenite takes place between the Ac_1 and Ac_3 temperatures which represent, respectively, the temperature at which the austenite formation starts and ends. The transformation start temperature Ac_1 is defined as the temperature at which the linear thermal expansion first deviates from linearity. This behaviour is caused by volume contraction associated with austenite formation which first compensates and then reverses the normal expansion of the steel due to the increase in temperature. Location of the point at which the deviation occurs is obtained by extrapolating the linear portion of the thermal expansion curve (*"tangent"* method). Likewise, transformation finish temperature Ac_3 is determined by extrapolating the linear portion of the curve after transformation [24]. However, for better determination of the critical points, it was applied also the *"first differential"*, evaluating the first derivative of the dilatometric curves. Table 4 shows the values of Ac_1 and Ac_3 calculated, whereas Fig. 4(a) describes the Continuous Heating Transformation (CHT) diagram for the steel employed in this work.

Table 4. Critical transformation temperatures for just quenched samples evaluated from dilatometric curves at different heating rates. The coefficient of Variation (CV) shows a little dispersion of experimental data obtained

Critical temperatures of austenitic transformation of 18NiCrMo5				
Heating Rate [K/s]	**A_{C1} [K]**	**CV [%]**	**A_{C3} [K]**	**CV [%]**
100	1001	0.99	1124	0.41
300	1004	1.06	1129	0.50
500	1010	0.28	1134	0.25
700	1014	0.43	1140.65	0.31
1000	1017	0.14	1151.65	0.92
1200	991	0.29	1139.65	0.19
1500	978	0.14	1132	0.12
1700	964.65	0.22	1129	0.10
2000	956	0.30	1125	0.25
2200	947.65	0.07	1122	0.13
2600	941	0.30	1115.65	0.06
3000	932	1.37	1108.65	0.70

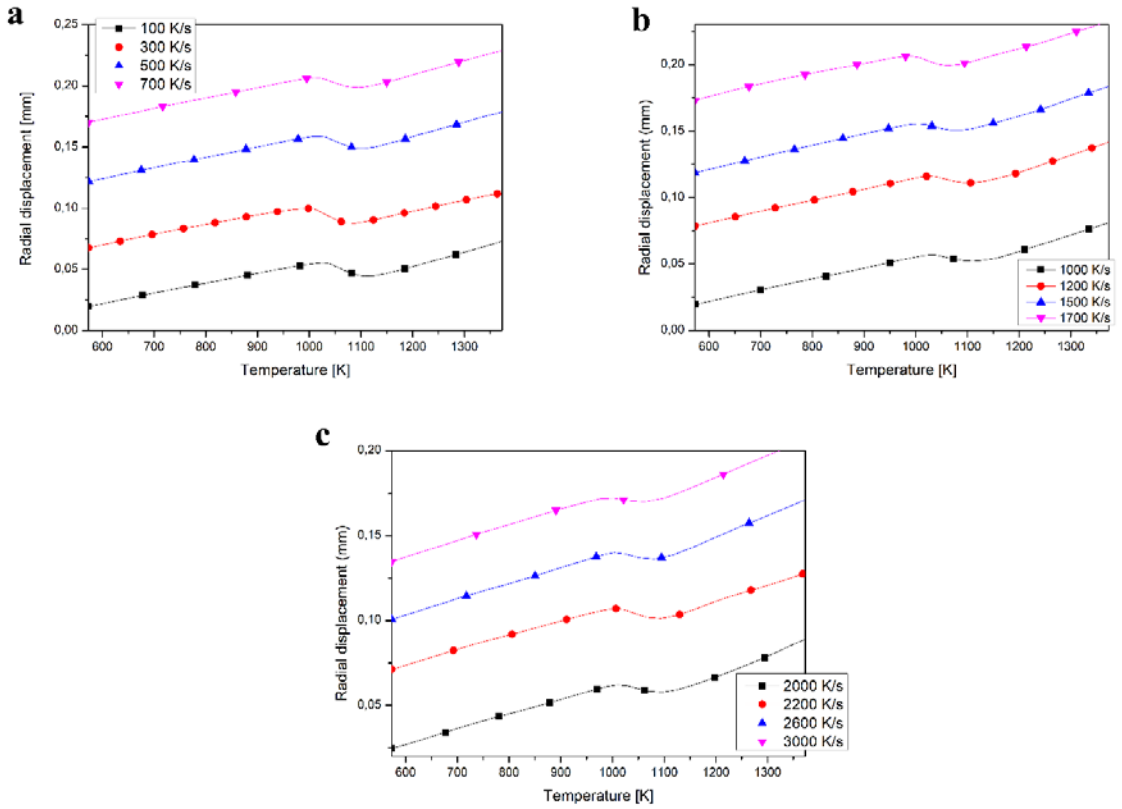

Fig. 3. (a-c) Dilatometric curves of the investigated steel for different heating rates measured during dilatometric tests

The temperature *vs.* heating rate plot, instead, is given in Fig. 4(b).

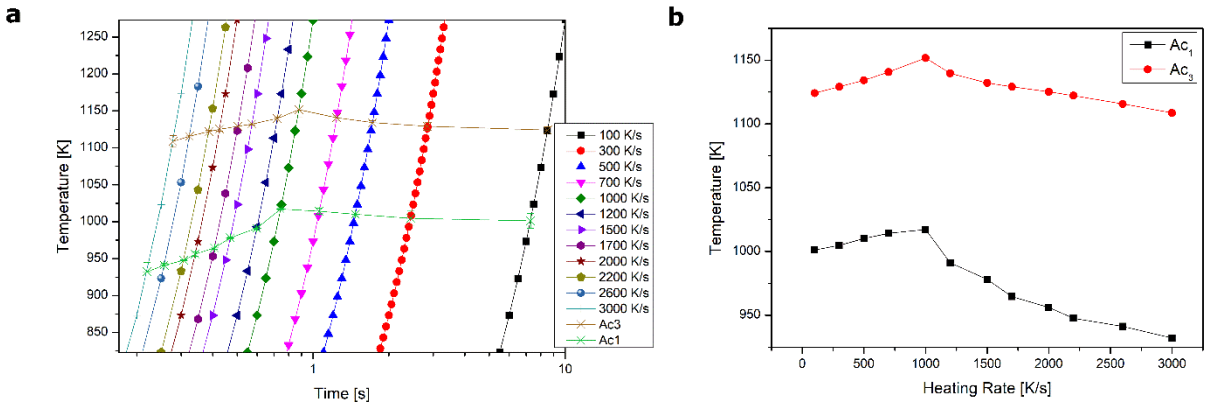

Fig. 4. a) Continuous Heating Transformation diagram of the investigated steel obtained using the critical transformation temperatures measured during dilatometric tests; b) Critical temperatures (Ac_1 and Ac_3) versus heating rate for the investigated steel.

From Figures 4(a) and (b), it can be oberved that the increase in the heating rate produced an increase of the finish temperature of austenitic transformation. However, this critical point reached a maximum at 1000 K/s and then decreased with the heating rate. The start temperature of austenitic transformation, also, increased until 1000 K/s and then decreased with heating rate. These behaviours suggested that martensite – austenite transformation at lower heating rates occurred with diffusive mechanism. Indeed, the increase of heating rate reduced the time for diffusion processes during the austenitization. These will

require, thus, greater energy and the process will complete at higher temperature than equilibrium condition, as shown by Han and Lee [25]. High heating rates involved displacive transformation, also defined "austenite reversion" [15] which dominates the austenitization process due to the increasingly inhibition of diffusion mechanism (especially of carbon). Therefore, critical points tend to decrease with heating rate until stabilizing when all the diffusion phenomena are fully inhibited [25]. A similar trend as function of the heating rate was observed for other low alloyed steel, for example medium Mn steel [25], martensitic stainless steel [26] and Fe-Ni-C alloy [15] and maraging steel [27]. The overall transformed volume fraction (*i.e.* the volume fraction of austenite formed) were determined through the lever rule for 4 heating rates (Fig. 5(a)). Despite the high heating rates employed in this work, the austenitization process was largely complete in all cases. The trend for 1700 K/s and 3000 K/s was quite similar. This is consistent with the fact that the transformation is displacive. Instead, the transformation curve for 1000 K/s is less steep compared to 100 K/s: then the kinetic of transformation for 1000 K/s is slower, resulting from low nucleation rate of austenite. This is linked to the fact that in diffusive transformation the greater is the heating rate the slower are the diffusion mechanisms during austenitization. Figure 5(b) shows the austenite formation time as a function of heating rate. This time decreased as the heating rate increased: in detail, this reduction is evident when the transformation is diffusive, whereas tends to be small/limited for a diffusionless transformation. For martensitic initial microstructure and diffusive transformation, the heating required for the austenite formation may first lead to tempering of the martensite and eventually to its decomposition into virtually carbon free ferrite and cementite or other carbide phases as stated by Lopes and Cota [28]. Indeed, Krauss [2] observed that, when austenite forms from martensite in steels, tempering during continuous heating can make the re-austenitisation process identical to that occurs in starting microstructure constituted by ferrite and cementite.

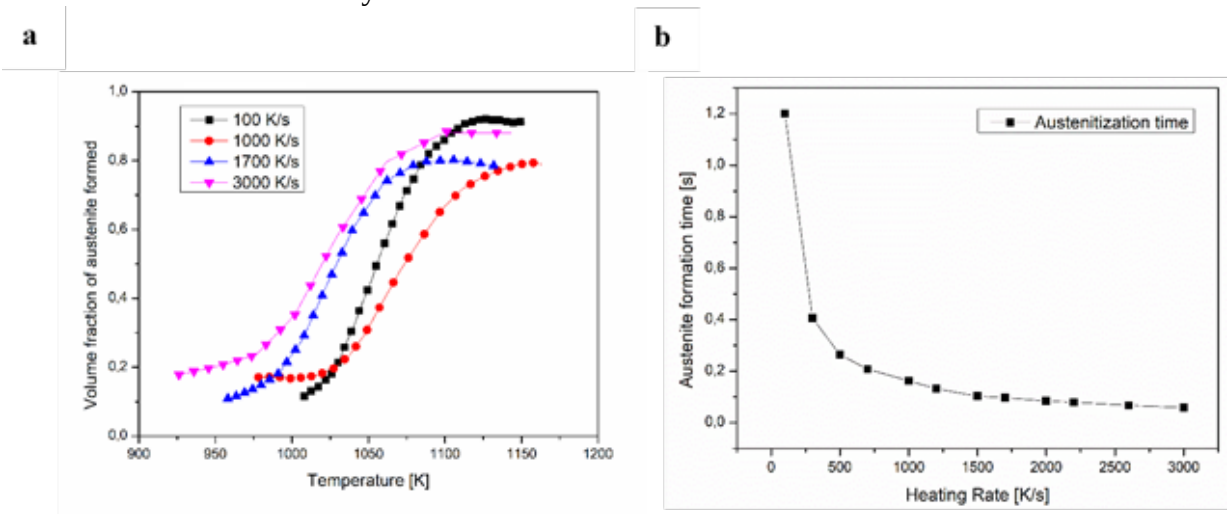

Fig. 5. a) Experimental austenitization curves for four heating rates obtained from dilatometric curves by applying the lever rule; and b) Heating rate vs. transformation time of the investigated steel evaluated from dilatometric curves of all heating rates

At slow heating rate, then, the tempering occurs and this prolonged heating could also lead to the coarsening of cementite particles as described by Mohanty *et al.* [29]. Austenite preferentially nucleates at the ferrite/cementite particle interfaces located on ferrite grain boundaries in the tempered martensite structure. Austenite soon envelops the cementite particle and the further growth is controlled by carbon diffusion in austenite. As time increases the amount of austenite increases due to the ferrite to austenite transformation and

cementite significantly decreases in size and density, indicating that austenite growth is accompanied by the dissolution of cementite particles [4].

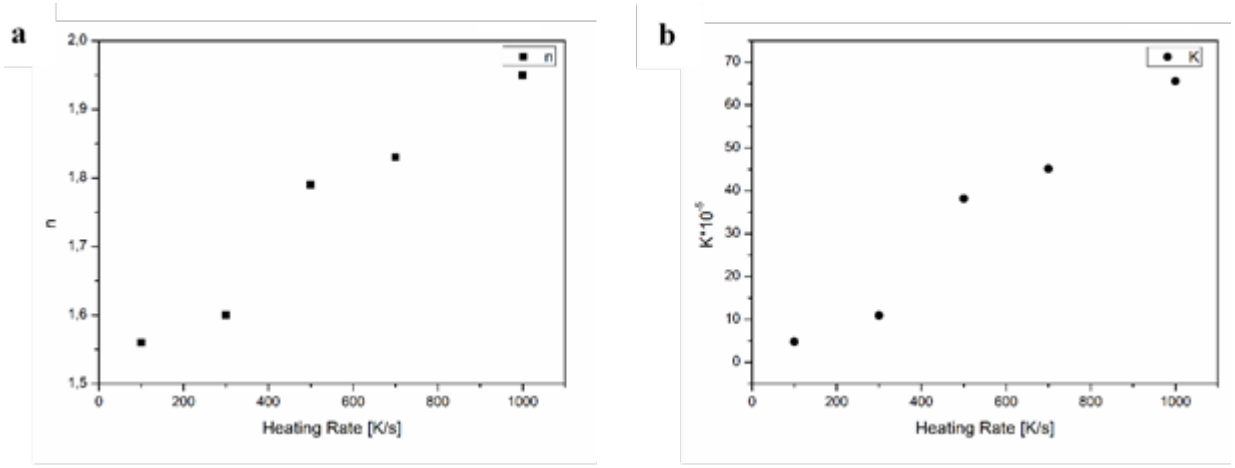

Fig. 6. a) Values of n and b) K as function of the heating rate calculated with JMAK equation for the 100-1000 K/s range of heating rates

As described by Zhao *et al.* [30], by the JMAK equation is possible to fit the austenite volume fraction as a function of time to evaluate values of *n* and *K*. Figure 6(a) shows that the exponent *n* is quite independent by the heating rate and its values lies between 1.7 and 1.95. Instead, the values of *K* increase with the heating rate (Fig. 6(b)). The parameter *K* represents the influence of the heating rate on the nucleation and growth rates of austenite. Then, the austenite formation rate is greater at high heating rates due to higher *K* parameter and lower transformation time [28].

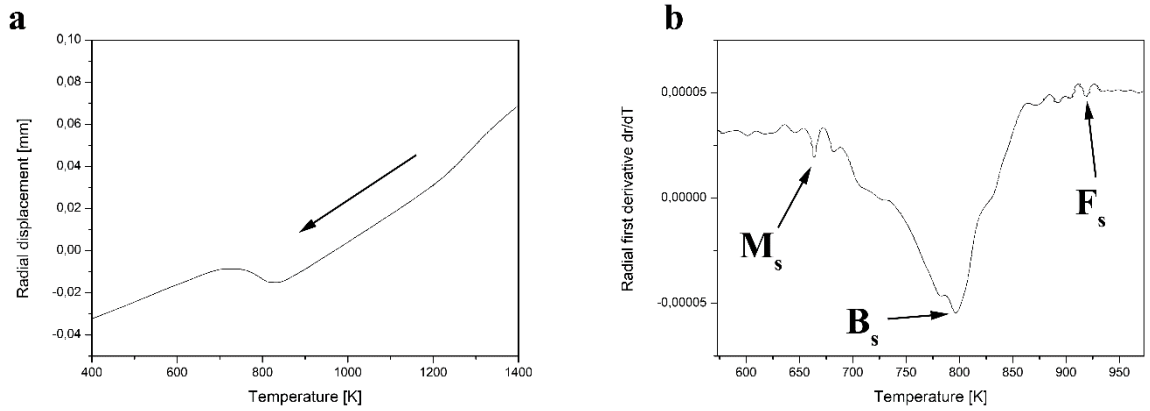

Fig. 7. (a) Example of dilatometric curve on cooling for the 100 K/s heating rate, (b) first derivative curve vs. temperature calculated from dilatometric curve on cooling for the 100 K/s heating rate. F_s: Ferrite start temperature, B_s: Bainite start temperature and M_s: Martensite start temperature

Microstructure of steel after dilatometric analysis was examined in order to verify the change of transformation mechanism with heating rate for the steel investigated. In particular, six samples were used with heating rates 100-300-1000-1700-2200-3000 K/s. The main aim was to highlight the microstructural differences between diffusionlessy and diffusively austenite. In order to evaluate all the phases obtained it was considered the dilatometric curve – an example is given in Fig. 7(a) – during cooling (that occured with the same rate) of

all samples. Moreover, this classification was simplified considering the first derivative curves (Fig. 7(b)) of dilatometric plot in which peaks of phase transformation can be clearly observed.

As shown in Figure 7(b), the formation of ferrite (F_s) starts to about 873 K whereas two peaks were observed at about 798 K and 663 K. The 798 K peak is originated from bainite (and matches the start of bainite transformation B_s), whereas the 663 K peak defines the martensite start temperature M_s. In this work, only the ferrite start temperature was considered and evaluated. Table 5 synthetizes the results obtained.

Table 5. Ferrite start temperature during cooling evaluated from dilatometric curves after heating in the range of 100 to 3000 K/s. It is shown also the coefficient of variation that indicates a little dispersion of the experimental data calculated

Heating Rate [K/s]	**F_s [K]**	**CV [%]**
100	873	1.01
300	876	0.95
1000	891	0,18
1700	903	0,25
2200	909	0,17
3000	913	0.50

Figure 8 shows the optical microstructures (x500) of samples after dilatometric test. In particular, four heating rates were chosen for this analysis: 100, 1000, 1700, 3000 K/s.

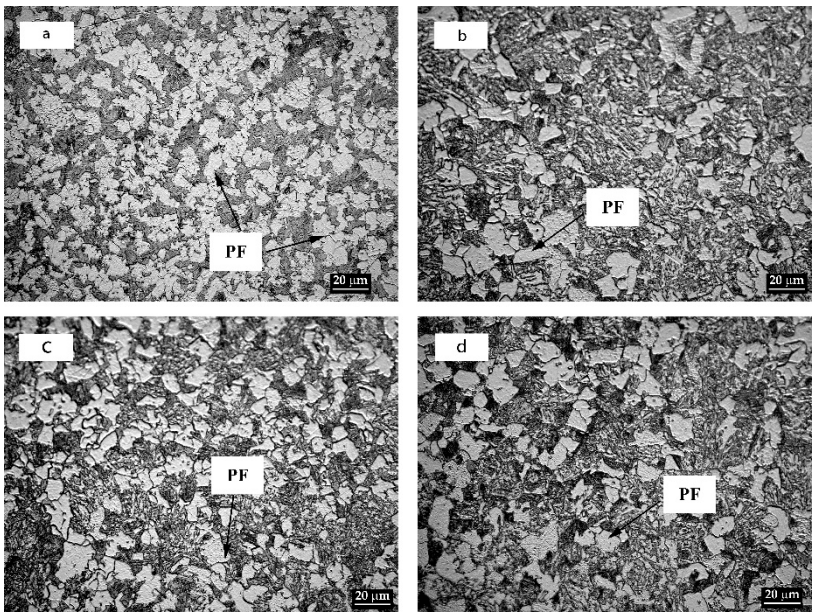

Fig. 8. Example of microstructures after dilatometric test for four different heating rates selected: (a) 100 K/s, (b) 1000 K/s, (c) 1700 K/s and (d) 3000 K/s. PF in all pictures means polygonal ferrite.

Besides ferrite, bainite and martensite were other microstructures observed. Ferrite was nucleated both at grain boundaries and inside of austenite grains and grew at relatively high temperature. In the bainite, instead, ferrite was firstly formed in elongated shape and the supersaturated austenite transformed into cementite either inside or outside of ferrite as stated by Kang *et al.* [22]. Small and few in number islands of martensite surrounded by bainite or ferrite were found in the samples.

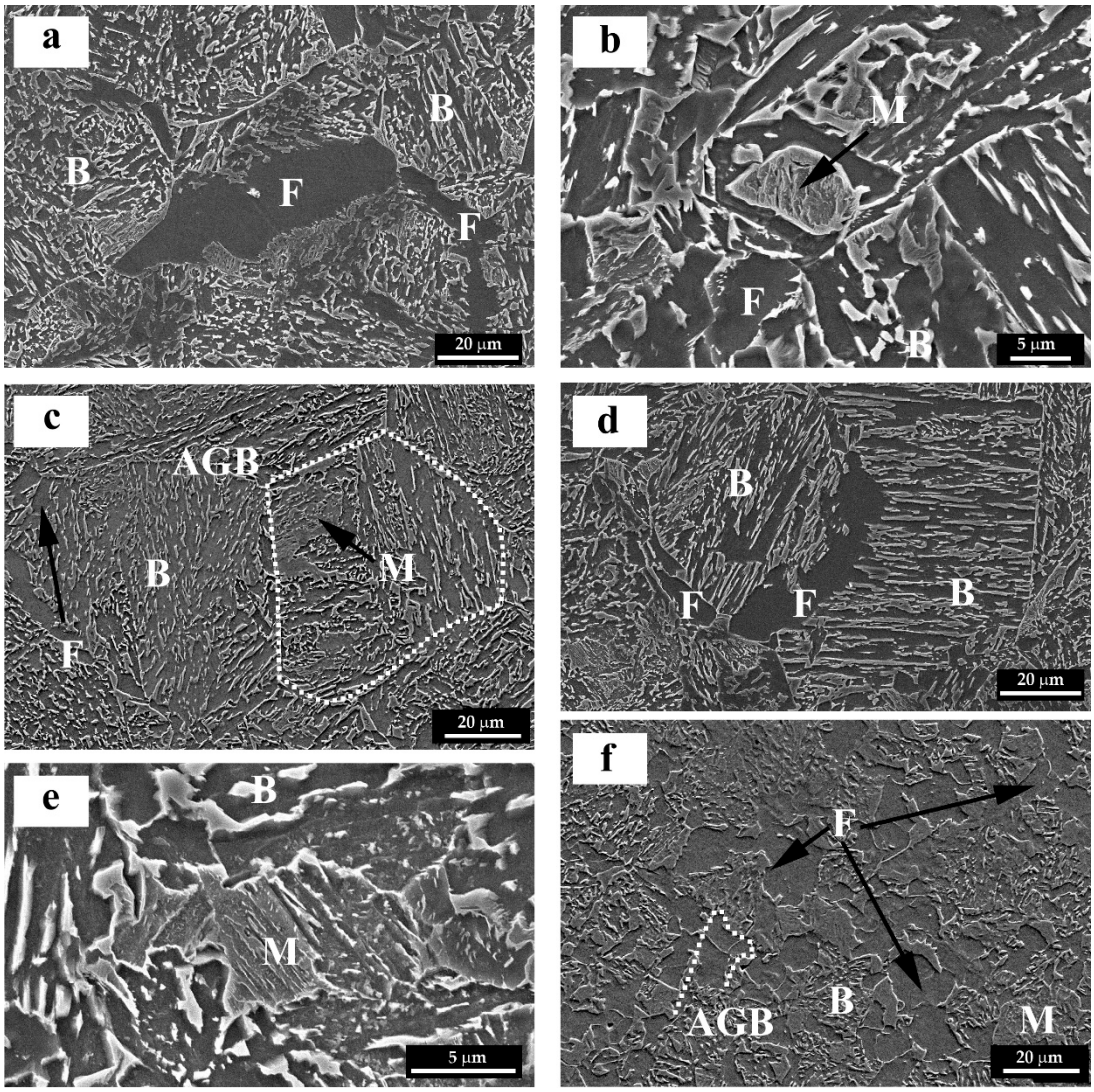

Fig. 9. Examples of SEM microstructures after dilatometric tests for four different heating rates: (a-b) 100 K/s, (c) 300 K/s, (d-e) 1000 K/s and (f) 3000 K/s

Samples obtained with low heating rate (100-300-1000 K/s) showed after cooling significant amount of bainite with martensitic areas inside (Fig. 9(a-e)). High dimension ferritic grains were also found for 100 and 1000 K/s (Fig. 9(a) and (d)). Another feature of samples heated with low heating rates was the low fraction of ferrite in microstructure compared to bainite. Moreover, it was possible to recognize prior austenite before cooling, especially in the sample heated with 300 K/s (Fig. 9(c)): the dashes lines highlighted (in a qualitative way) the austenite grain boundaries which shape appeared to be almost globular. This is the evidence of thermally activated mechanism which involves diffusion. Indeed, Han and Lee [25] showed that at low heating rate the austenite obtained is characterized by globular or equiaxed shape and low dislocation density.

Sample heated at 3000 K/s (Fig. 9(f)), instead, was mainly composed by high amount of ferritic grains with bainitc areas. The dashes lines described (in a qualitative way) prior austenite with lath shape grains. This suggested the occurrence of displacive mechanism as shown by Han and Lee [25]. The visible differences on microstructure for low and high heating rates samples, therefore, can suggest difference between austente prior microstructure.

TEM images of the samples heated at 100 K/s (a) and 3000 K/s (b) and cooled with the same rate are shown in Fig. 10. The main constituents were ferrite, the grey zones which form the matrix of the microstructure, and martensite forming the black areas.

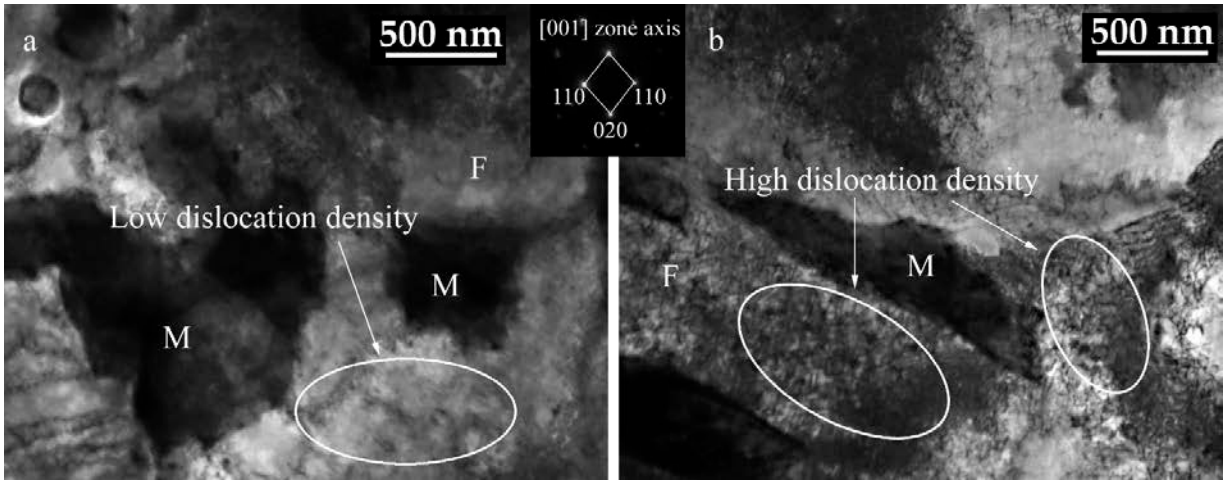

Fig. 10. Examples of TEM bright field images after dilatometric tests for two different heating rates: (a) 100 K/s and (b) 3000 K/s. F means Ferrite and M means Martensite

It was possible to observe that the sample heated at 3000 K/s and cooled showed a higher number of dislocations in comparison with the sample heated at 100 K/s and cooled. The $\alpha' \rightarrow \gamma$ transformation at high heating rates is carried out by cooperative rearrangment of atoms by displacive mechanism. This process is accompanied by formation of dislocations in austenite microstructure as described by Maksimkin [31]. During cooling there is reduction and rearrangement of dislocations. However, part of dislocations still remains in ferritic structure. The presence of high dislocation density and stored energy in austenite obtained at high heating rates is generally recognized as the enhancing effect on austenite-ferrite transformation kinetics on cooling. More specifically, Hanlon *et al.* [32] found that the transformation start temperature F_s is shifted to higher temperature due to the additional stored energy of the deformed austenite with high dislocation density. This is in agreement with the data in Table 5. It is shown that F_s shifted to higher temperature with increasing the heating rates: the maximum temperature difference is 313 K suggesting that at 3000 K/s the austenite had fine microstructure obtained without any long range atomic movement (*i.e.* diffusion). This is an essential characteristic of displacive transformation. Morover, the high number of dislocation in austenite at high heating rates increase the grain/subgrain boundary area which acts as ferrite nucleation sites, promoting the nuleation of ferrite grains and the subsequent grain refiniment of ferrite [33]. Then, Crooks *et al.* [34] found that the final fraction of ferrite increase whereas the ferrite grain size decrease. This effect is shown in Fig. 9(f). In the sample heated at 3000 K/s there is large amount of ferrite with smaller grain size compared to samples heated at 100 K/s (see Fig. 9(a)) and 300 K/s (see Fig. 9(c)) with lower amount of ferrite with larger size.

4. Conclusion

In this study, it was analyzed the effect of heating rate on the austenitization of 18NiCrMo5 steel with a prior martensitic microstructure.

For this aim dilatometric tests were conducted choosing 12 heating rates and the same cooling rate for all tests. After cooling the samples were characterized with OM, SEM and TEM.

According to experimental findings the following conclusion can be drawn:

1. Regarding critical point Ac_1 and Ac_3 tempeatures increased with heating rate up to maximum value and then decrease;
2. Austenite formation at low heating rates involved the diffusive mechanism leading to globular austenite with low amount of dislocations;
3. At high heating rate austenite transformation had the displacive mechanism defined austenite reversion. The obtained austenite showed lath-shaped and deformed grains with high density of dislocations;
4. The dislocation substructures typical of austenite obtained at high heating rates increased the stored energy and the number of nucleation sites accelerating the austenite-ferrite transformation on cooling.

Acknowledgements. *No external funding was received for this study.*

References

[1] Oliveira FLG, Andrade MS, Cota AB. Kinetics of austenite formation during continuous heating in a low carbon steel. *Materials Characterization.* 2007;58(3): 256-261.
[2] Krauss G. *Steels: Heat Treatment and Processing Principles*. Ohio: ASM International; 1990.
[3] Thibaux P, Tenier AM, Xhoffer C. Carbon diffusion measurement in austenite in the temperature range 500-900°C. *Metallurgicial and Materials Transaction A.* 2007;38A(6): 1169-1176.
[4] Speich GR, Szirmae A. Formation of austenite from ferrite and ferrite-carbide aggregates. *Transaction of the Metallurgical Society of AIME*. 1969;245: 1063-1073.
[5] Roberts GA, Mehl RF. The mechanism and the rate of formation of austenite from ferrite-cementite aggregates. *ASM Transaction*. 1943;31: 613-650.
[6] Judd RR, Paxton HW. Kinetics of austenite formation from a spheroidized ferrite-carbide aggregate. *Transaction of the Metallurgical Society of AIME*. 1968;242: 206-215.
[7] Gridnev VN, Trefilov VI. Over the reversability of the martensitic transformation in Fe-C alloys during heating. *Doklady Akademii Nauk SSSR*. 1954;95: 741-743.
[8] Caballero FG, Capdevila C, García de Andreís C. Influence of scale parameters of pearlite on the kinetics of anisothermal pearlite to austenite transformation in a eutectoid steel. *Scripta Materialia*. 2000;42(12): 1159-1165.
[9] San Martin D, Rivera Díaz del Castillo PEJ, García de Andreís C. In situ study of austenite formation by dilatometry in a low carbon microalloyed steel. *Scripta Materialia*. 2008;58(10): 926-929.
[10] Shinozaki T, Tomota Y, Fukino T, Suzuki T. Microstructure evolution during reverse transformation of austenite from tempered martensite in low alloy steel. *ISIJ International*. 2017;57(3): 533-539.
[11] Kinoshita S, Ueda R. Some observations on formation of austenite grains. *Transactions of the Iron and Steel Institute of Japan*. 1974;14: 411-418.
[12] Homma R. Studies on austenite grain of 3.5%Ni-Cr- Mo-V steel. *Transactions of the Iron and Steel Institute of Japan*. 1974;14: 434-443.
[13] Rudnev VI, Loveless DL, Cook RL, Black MR. *Handbook of induction Heating*. New York: Marcel Dekker ed.; 2003.
[14] Castro Cerda FM, Sabirov I, Goulas C, Sietsma J, Monsalve A, Petrov RH. Austenite formation in 0.2% C and 0.45% C steels under conventional and ultrafast heating. *Materials & Design*. 2017;116: 448-460.
[15] Apple CA, Krauss G. The effect of heating rate on the martensite to austenite transformation in Fe-Ni-C alloys. *Acta Metallurgica*. 1972;20(7): 849-856.

[16] Kokosza A, Pracyna J, Bała P, Dziurka R. The influence of continuous heating rate on the austenite formation in the medium carbon TRIP steel. *Archives of Materials Science and Engineering*. 2013;62(1): 22-27.
[17] Garcia de Andrés C, Caballero FG, Capdevila C, Álvarez LF. Application of dilatometric analysis to the study of solid–solid phase transformations in steels. *Materials Characterization*. 2002;48(1): 101-111.
[18] Dykhuizen RC, Robino CV, Knorovsky GA. A method for extracting phase change kinetics from dilatation for multistep transformations: austenitization of a low carbon steel. *Metallurgical and Materials Transactions B*. 1999;30(1): 107-117.
[19] Katsamas AI. A computational study of austenite formation kinetics in rapidly heated steels. *Surface and Coatings Technology*. 2007;201(14): 6414-6422.
[20] Spezzapria M, Settimi AG, Pezzato L, Novella MF, Forzan M, Dughiero F, Bruschi S, Ghiotti A, Brunelli K, Dabalà M. Effect of prior microstructure and heating rate on the austenitization kinetics of 39NiCrMo3 steel. *Steel Research International*. 2016;87: 1-10.
[21] Mehta M, Oakwood T. *Develpment of a standard methodology for the quantitative measurement of steel phase transformation kinetics and dilatation strains using dilatometric methods,QMST (TRP 0015).* US Department of Energy. 2004.
[22] Kang HU, Park BJ, Jang JH, Jang KS, Lee KJ. Determination of the continuous cooling transformation diagram of a high strength low alloyed steel. *Metals and Materials International*. 2016;22(6): 945-955.
[23] Kitahara H, Ueji R, Tsuji N, Minamino Y. Crystallographic features of lath martensite in low alloy steel. *Acta Materialia*. 2006;54(5): 1279-1288.
[24] Gunabalapandian K, Samanta S, Ranjan R, Singh SH. Investigation of austenitization in low carbon microalloyed steel during continuous heating. *Metallurgical and Materials Transaction A*. 2017;48(5): 2099-2104.
[25] Han J, Lee YK. The effects of the heating rate on the reverse transformation mechanism and the phase stability of reverted austenite in medium Mn steels. *Acta Materialia*. 2014;67: 354-361.
[26] Lee YK, Shin HC, Leem DS, Choi JY, Jin W, Choi CS. Reverse transformation mechanism of martensite to austenite and amount of retained austenite after reverse transformation in Fe-3Si-13Cr-7Ni (wt-%) martensitic stainless steel. *Materials Science and Technology*. 2003;19(3): 393-398.
[27] Sinha PP, Sivakumar D, Babu NS, Tharian KT, Natarajan A. Austenite reversion in 18 Ni Co-free maraging steel. *Steel Research International*. 1995;66(11): 490-494.
[28] Lopes MMB, Cota AB. A study of isochronal austenitization kinetics in a low carbon steel. *REM: Revista Escola de Minas*. 2014;67(1): 61-66.
[29] Mohanty RR, Girina OA, Fonstein NM. Effect of heating rate on the austenite formation in low carbon high strength steel annealed in the intercritical region. *Metallurgical and Materials Transaction A*. 2011;42: 3680-3690.
[30] Zhao JZ, Mesplont C, De Cooman BC. Calculation of the phase transformation kinetics from a dilatation curve. *Journal of Materials Processing and Technology*. 2002;129(1-3): 345-348.
[31] Maksimkin OP. Phase diffusionless γ↔α transformation and their effect on physical, mechanical and corrosion properties of austenitic stainless steel irradiated with neutrons and charge particles. *IOP Conference Series: Materials Science and Engineering*. 2016;130: 1-13.
[32] Hanlon DN, Sietsma J, van der Zwaag S. The effect of plastic deformation of austenite on the kinetics of subsequent ferrite formation. *ISIJ International*. 2001;41(9): 1028-1036.
[33] Xu PJ, Tomota Y, Lukáš P, Muránsky O, Adachi Y. Austenite-to-ferrite transformation in low alloy steels during thermomechanically controlled process studied by in situ neutron diffraction. *Materials Science and Engineering A*. 2006;435-436: 46-53.

[34] Crooks MJ, Garrar-Reed AJ, Vander Sande JB, Owen WS. The isothermal austenite-ferrite transformation in some deformed vanadium steels. *Metallurgical and Materials Transaction A.* 1982;13(8): 1347-1353.